Kidney International, Vol. 68 (2005), pp. 1048–1060

Expression of HIV-1 genes in podocytes alone can lead to the full spectrum of HIV-1–associated nephropathy

JIANYONG ZHONG, YIQIN ZUO, JI MA, AGNES B. FOGO, PAUL JOLICOEUR, IEKUNI ICHIKAWA, and TAIJI MATSUSAKA

Department of Pediatrics, Vanderbilt University Medical Center, Nashville, Tennessee; Department of Medicine, Vanderbilt University Medical Center, Nashville, Tennessee, Department of Pathology, Vanderbilt University Medical Center, Nashville, Tennessee; Department of Pediatrics, Institute of Medical Science, Tokai University, Isehara, Kanagawa, Japan; Department of Nephrology, Huashan Hospital, Fudan University, Shanghai, China; and Laboratory of Molecular Biology, Clinical Research Institute of Montreal, Montreal, Quebec, Canada

Expression of HIV-1 genes in podocytes alone can lead to the full spectrum of HIV-1–associated nephropathy.

Background. Human immunodeficiency virus (HIV)-1–associated nephropathy (HIVAN) is characterized by collapsing focal and segmental glomerulosclerosis (FSGS) and microcystic tubular dilatation. HIV-1 infection is also associated with other forms of nephropathy, including mesangial hyperplasia. Since HIV-1 gene products are detected in podocytes and other renal cells, it remains uncertain whether podocyte-restricted HIV-1 gene expression can account for the full spectrum of renal lesions involving nonpodocytes.

Methods. To define the role of podocyte-restricted HIV-1 gene expression in the progression of HIVAN, we generated transgenic mice that express nonstructural HIV-1 genes selectively in podocytes.

Results. Four of the seven founder mice developed proteinuria and nephropathy. In a subsequently established transgenic line, reverse transcription-polymerase chain reaction (RT-PCR) analysis detected mRNAs for *vif*, *vpr*, *nef*, and spliced forms of *tat* and *rev*, but not *vpu*, in the kidney. In situ hybridization localized HIV-1 RNA to the podocyte. Transgenic mice on FVB/N genetic background exhibited cuboidal morphology of podocytes with reduced extension of primary and foot processes at 2 weeks of age. After 3 weeks of age, these mice developed massive and nonselective proteinuria with damage of podocytes and other glomerular cells and, after 4 weeks of age, collapsing FSGS and microcystic tubular dilatation. In marked contrast, transgenic mice with C57BL/6 genetic background showed either normal renal histology or only mild mesangial expansion without overt podocyte damage.

Conclusion. The present study demonstrates that podocyte-restricted expression of HIV-1 gene products is sufficient for the development of collapsing glomerulosclerosis in the setting of susceptible genetic background.

Key words: HIV-1–associated nephropathy, proteinuria, podocyte damage.

Received for publication December 21, 2004
and in revised form March 22, 2005
Accepted for publication April 8, 2005

Podocytes, or glomerular visceral epithelial cells, play a critically important role as the filtration barrier of the glomerulus [1]. Moreover, it has been observed in many clinical and experimental settings that podocyte injury precedes glomerulosclerosis, a morphologic hallmark of end-stage renal failure [2–5]. Recent studies in humans and gene-targeted mice revealed that mutations in molecules which have important roles in podocytes, including nephrin, podocin, CD2-associated protein and α-actinin-4, result in proteinuria and glomerulosclerosis [6–12]. These findings indicate that injury of podocytes can trigger the sequence of pathologic events leading to glomerulosclerosis [10, 13–15].

Human immunodeficiency virus (HIV)-1–associated nephropathy (HIVAN) affects up to 10% of HIV-1–infected individuals with a marked racial predilection for black and Hispanic people [5, 16–21]. HIVAN is characterized by severe podocyte alterations, heavy proteinuria, and rapid progression to end-stage renal failure. Pathologically, HIVAN is characterized at late stage by collapsing focal and segmental glomerulosclerosis (FSGS) and tubulointerstitial changes, including microcystic tubular dilation. Podocytes are dedifferentiated with loss of synaptopodin and Wilms tumor (WT)-1 proliferate and undergo apoptosis [22–24]. HIV-1 mRNA and DNA have been detected in epithelial cells, including podocytes, parietal epithelial cells, and tubular cells, in HIVAN [25–28]. Although HIVAN is the most common renal complication in HIV-1–infected patients, HIV-1 infection is also associated with other forms of renal diseases, including minimal change nephropathy, mesangial hyperplasia, and immune-mediated glomerulonephritis [16, 19, 29, 30]. The latter lesions are more common in HIV-1–infected Caucasians [29].

Studies using transgenic animals have provided important insights into HIVAN pathogenesis. Tg26, a transgenic mouse line carrying HIV-1 proviral DNA defective

for *gag* and *pol*, developed nephropathy similar to HIVAN in humans [31, 32]. In these mice, the transgene expression is driven by the authentic viral promoter, LTR, and occurs in various organs [31]. In the kidney, transgene expression was detected in podocytes, glomerular parietal epithelial cells, and various parts of tubular cells [26, 33, 34]. Similar to HIVAN in humans, glomeruli in Tg26 transgenic mice showed collapsing FSGS, accompanied by proliferation, dedifferentiation, and apoptosis of podocytes. The tubulointerstitial changes included microcystic dilatation, proliferation, and apoptosis of tubular cells [33, 34]. Renal cross-transplantation experiments between transgenic and wild-type mice indicated that HIV gene products generated in the kidney cause nephropathy independently of circulating viral proteins or dysregulated cytokines [34]. The same transgene construct also caused nephropathy similar to human HIVAN in rats [35, 36]. These studies in humans and animal models indicate that HIV-1 gene products generated in renal cells, including podocytes and tubular cells, directly cause nephropathy.

In addition, other transgenic lines, CD4C/HIV and CD4C/simian immunodeficiency virus (SIV), respectively, expressing HIV Nef or SIV Nef under the control of the CD4C regulatory elements, developed segmental glomerulosclerosis, tubulointerstitial nephritis, and microcystic dilatation [37–41]. These CD4C sequences represent a chimeric construct of the human CD4C promoter and the mouse CD4 enhancer and have been shown to drive expression of surrogate genes in mature and immature $CD4^+$ T cells and in cells of the macrophage/myeloid lineage [37, 42–44]. The interstitial nephritis in this line was alleviated by an Iκ-B kinase inhibitor, in association with reduction in regulated upon activation, normal T-cell expressed and secreted (RANTES) [45], suggesting that inflammatory cytokines induced by HIV-1 gene products may be involved in the development of the renal disease in these transgenic mice.

In the present study, to further delineate the direct effect of HIV-1 genes on podocytes, and to define the role of podocyte dysregulation in the progression of HIVAN, we have generated transgenic mice expressing HIV-1 genomic DNA selectively in podocytes, utilizing the promoter of the mouse nephrin gene, *Nphs1*.

METHODS

Generation of transgenic mice

The transgene was constructed from mutant B, a mutant HIV-1 genome used in a previous study [45]. Mutant B was derived from NL4-3 (GeneBank M1992) and has a point mutation in *env*. The BssHII-Aat II fragment of mutant B, which contains all HIV-1 coding regions, nucleotide (nt) 711-9562, and a polyadenylation signal of SV40, was subcloned into pBR322. From this DNA, the portion spanning from Sph1 (nt 1443) to Bal1 (nt 4551)

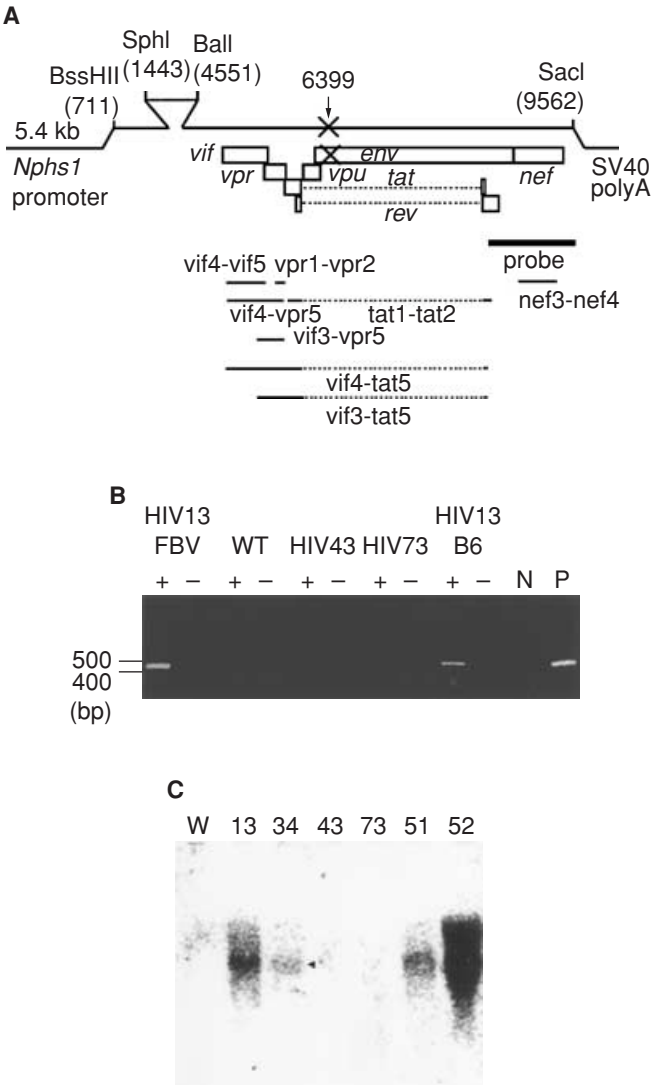

Fig. 1. Generation of podocyte specific HIV-1 transgenic mice. (*A*) Structure of the transgene. The transgene, depicted by the top line, consisted of a 5.4 kb *Nphs1* promoter, a fragment of NL4-3 proviral DNA and a poly A signal from SV40 DNA. Some key restriction enzyme sites and nucleotide numbers (nt) according to the GeneBank M1992 are shown. The NL4-3 DNA fragment spans nt 711-9562, with a deletion of nt 1443-4551 (*gag* and *pol* are disrupted) and a point mutation at 4551 in *env* as depicted by X. The resultant transgene encodes *vif*, *vpr*, *vpu*, *tat*, *rev*, and *nef*. The position of each gene is shown by open boxes. Dashed lines represent the intron of *tat* and *rev*. The bold bars show the positions of the probes for in situ hybridization and Northern blot analysis. The thin lines shown below depict positions of mRNAs detected by reverse transcription-polymerase chain reaction (RT-PCR) in the kidney of HIV13 transgenic mice. The portion of the intron of *tat* and *rev,* shown by dashed lines, was not detected by RT-PCR. (*B*) Representative results of RT-PCR for HIV-1 mRNA. +, reaction with RT; −, reaction without RT; N, negative control using wild-type genomic DNA as a template; P, positive control using transgenic genomic DNA as a template. HIV-1 mRNA was detected in the RNA from the kidneys of HIV13FBV and HIV13B6, but not in those from HIV43, HIV73 or wild-type mice. (*C*) Northern blot analysis for HIV-1 mRNA in the founder transgenic mice. A ^{32}P-labeled DNA fragment including *nef* was used as a probe [shown in (A)]. Specific signal was detected in HIV13, HIV51, and HIV52, and faintly in HIV34 (arrowhead), but not in HIV43, HIV73, or wild-type mice.

Table 1. Polymerase chain reaction (PCR) primers used in this study

Name	Primer sequence (5′-3′)	Position
vif4	GTACTTGGCACTAGCAGCATT	5073–5094
vif3	GCAAGTAGACAGGATGAGGATT	5478–5498
vif5	CTTGTTCCATCTGTCCTCTGT	5568–5548
vpr1	TGAAACTTACGGGGATACTTGG	5699–5720
vpr2	GTCGAGTAACGCCTATTCTGC	5814–5794
vpr5	CCCAAGTATCCCCGTAAGTTT	5721–5701
tat1	AGACTAGAGCCCTGGAAGCATC	5848–5869
tat5	CTTCTATTCCTTCGGGCCTGTC	8417–8396
rev1	CGTCCCAGATAAGTGCTAAGGATC	8489–8466
vpu1	AAAGAGCAGAAGACAGTGGCAAT	6200–6222
vpu2	CATTTCCACCCCCATCTCCACA	6270–6249
nef3	TAAGGGAAAGAATGAGACGAGC	8833–8854
nef4	ACTCTAACACTTCTCTCTCAGG	9312–9333
nef6	GGAAAGAATGAGACGAGCTG	8837–8856
nef8	ATTCCATGCAGGCTCACAGG	9285–9304

was deleted to disrupt *gag* and *pol*. The resultant fragment was combined with a 5.4 kb promoter region of *Nphs1* (Fig. 1A).

The transgene DNA was microinjected into fertilized eggs obtained from mating between DBF1 and C57BL/6 mice. Transgenic mice were identified by polymerase chain reaction (PCR) performed on genomic DNA from the tail, using primers, nef3 and nef4. The genotype was confirmed by Southern analysis. Founder transgenic mice were mated with wild-type C57BL/6N or FVB/N mice.

Detection of the transgene expression

PolyA-RNA was isolated from the whole kidney using Micro-Fast Track Kit (Invitrogen, Carlsbad, CA, USA). Northern analysis was performed using a DNA probe (nt 8465-9562) (Fig. 1A). The following primer sets were used to detect HIV-1 gene products by reverse transcription (RT)-PCR: vif4 and vif5, vif4 and vpr5, vif3 and vpr5, vpr1 and vpr2, tat1 and rev1, vif4 and tat5, vif3 and tat 5, nef3 and nef4, nef6 and nef8, and vpu1 and vpu2. The positions of these primers are listed in Table 1.

In situ hybridization was carried out using an RNA probe that covers a 3′ end of the HIV-1 coding region (nt 8465-9562) (Fig. 1A) as previously reported [46]. ^{35}S-labeled sense and antisense probes were generated using MAXISCRIPT™ In Vitro Transcription Kit (Ambion, Austin, TX, USA). Each probe was sheared by alkaline hydrolysis to yield RNA about 150 bp in length.

Animal experiments

The Animal Experimentation Committee of Tokai University Medical School and the Institutional Animal Care and Use Committee of Vanderbilt University Medical Center approved the protocol, in accordance with the principles and procedures outlined in the National Institute of Health Guide for the Care and Use of Laboratory Animals.

Fourteen HIV13FVB mice and 14 wild-type littermates were followed up to 18 weeks of age. These were sacrificed when they showed clinical signs of wasting. In addition, for histologic analysis, the following numbers of HIV13FVB mice and wild-type littermates, respectively, were sacrificed at the indicated time points: 4 and 5, at 1 week of age, 4 and 5 at 2 weeks of age, 18 and 14 at 3 weeks of age, and 8 and 5 at 4 weeks of age.

Fifty-five HIV13B6 mice and 50 wild-type littermates were followed up to 18 weeks of age for the survival rate. The following numbers of HIV13B6 mice and wild-type littermates, respectively, were analyzed for histology at the indicated time points: 6 and 6 at 2 weeks of age, 2 and 2 at 5 weeks of age, 2 and 2 at 6 weeks of age, 5 and 5 at 9 weeks of age, and 12 and 12 after 6 months of age.

Twenty-four–hour urine specimens were collected in metabolic cages. Concentrations of total protein and creatinine in the urine were determined with an automatic analyzer (SRL, Tokyo, Japan). Urine samples (2 μL) were analyzed by sodium dodecyl sulfate-polyacrylamide gel electrophoresis (SDS-PAGE) using 2% to 15% gradient gel.

Morphologic analysis

For routine histology and immunostaining, kidneys were fixed in 4% buffered paraformaldehyde (PFA) and embedded in paraffin. For transmission electron microscopy, kidneys were fixed in 2.5% glutaraldehyde/0.05 mol/L phosphate buffer at 4°C for overnight, washed in 0.1 mol/L phosphate buffer, further fixed in 1% OsO_4/0.05 mol/L phosphate buffer and dehydrated in serial graded ethanol and acetone. For scanning electron microscopy, tissue pieces were fixed in glutaraldehyde, dehydrated in ethanol, fractured with a knife, prepared with a critical point drier, and coated with gold using an ion sputter. The fractured surface was observed with 15 kV acceleration voltage.

Glomerular maturity index was determined at 2 weeks of age as previously described [46].

Immunostaining

The following primary antibodies were used in the present study: monoclonal antirat synaptopodin (Progen, Heidelberg, Germany), monoclonal antidesmin (1:50) (DakoCytomation, Kyoto, Japan), monoclonal anti-Ki-67 (1:200) (Novocastra Laboratories Ltd., Newcastle, UK), rabbit antihuman WT-1 (1:100) Santa Cruz Biotechnology, Santa Cruz, CA, USA), rabbit antikeratin/cytokeratin (1:100) (Nichirei, Tokyo, Japan), goat antimouse IgG (1:20) (ICN, Aurora, OH, USA), goat antimouse IgM (1:50) (ICN), goat antimouse IgA (1:2000) (ICN), goat antimouse complement C3 (1:1000) (ICN), and goat antimouse fibrinogen antibody (Nordic Immunology, Tilburg, The Netherlands). In addition, the

Table 2. Summary of HIV-1 founder transgenic mice

Mouse	Gender	Urinary protein/ creatinine(age)[a]	Renal histology	Survival time	Transgene expression[b]	Renal histology of transgenic offspring
HIV13	M	22.9 (6 months)	Mild FSGS	>13 months	(+)	FSGS
HIV34	F	**13.1 (6 weeks)**	ND	10 months	(+)	FSGS
HIV42	F	ND	ND	30 days	ND	No offspring
HIV43	M	12.8 (6 months)	Normal	>13 months	(−)	Normal
HIV51	M	25.3 (6 months)	Normal	>6 months	(+)	No offspring
HIV52	M	**44.7 (6 months)**	FSGS	>6 months	(+)	No offspring
HIV64	F	**62.7 (6 weeks)**	FSGS	52 days	(+)	No offspring
HIV73	F	12.6 (6 months)	Normal	>13 months	(−)	Normal

FSGS is focal segmental glomerulosclerosis; ND is not determined.
[a]The concentration ratio of total urinary protein (mg/mL) to urinary creatinine (mg/mL). Values in bold letters indicate significant elevation compared to age- and gender-matched wild-type mice.
[b]Transgene expression determined by reverse transcription-polymerase chain reaction (RT-PCR) on total RNA extracted from the kidney.

following antibodies were obtained from the NIH AIDS Research and Reference Reagent Program and used in the present study: monoclonal anti-NEF (AG11 and AE6), monoclonal anti-TAT (NT3 2A4.1 and NT3 5A 5.3), monoclonal anti-VIF (319), monoclonal anti-REV (1G7), monoclonal anti-TAT (1D9), rabbit anti-VIF and rabbit anti-VPR. For synaptopodin, desmin, Ki-67, and WT-1, tissues were heated by microwave. For cytokeratin, tissues were pretreated with 0.1% trypsin for 10 minutes at 37°C. No staining was detected without primary antibodies.

Statistics

Results are expressed as mean ± standard error. Data were analyzed by unpaired *t* test. Differences were considered to be statistically significantly at $P < 0.05$.

RESULTS

Generation of transgenic mice expressing HIV-1 genes in the kidney

We constructed a transgene by combining a promoter fragment of *Nphs1*, which directs podocyte-specific expression, and HIV-1 proviral DNA with mutations in *gag*, *pol*, and *env*. The resulting transgene encodes *vpr*, *vif*, *tat*, *rev*, *nef*, and *vpu*.

We obtained eight founder transgenic mice (Table 2). One founder mouse, coded HIV42, showed severe growth retardation and died at 30 days of age before analysis. The remaining seven mice were analyzed. The development of nephropathy in Tg26 line has been reported to be dependent on FVB/N genetic background. We, therefore, mated these founder mice with both C57BL/6 and FVB/N mice.

Overall, of the seven transgenic mice analyzed, four developed nephropathy. One founder mouse, HIV13, did not show proteinuria and survived for more than 13 months. Histologic analysis at 13 months of age showed focal intratubular casts and sclerosis in a few glomeruli. The HIV13 founder mouse generated many transgenic offspring, which were analyzed in detail as described below. Most transgenic mice generated by mating HIV13 and FVB/N mice (designated as HIV13FVB) developed collapsing FSGS, whereas those generated by mating with C57BL/6 mice (designated as HIV13B6) showed no or very mild renal lesions.

Two other founder transgenic mice, HIV64 and HIV52, developed proteinuria and nephropathy similar to HIV13FVB. No offspring was obtained from these mice. HIV34 mice showed slightly elevated urinary protein/creatinine ratios at 6 weeks of age and died at 10 months of age without morphologic analysis. Two transgenic offspring were obtained from mating with C57BL/6 mice. These showed proteinuria after 7 weeks of age, and morphologic analysis done at 2 and 12 months of age revealed nephropathy similar to that in HIV13FVB.

Three other founder transgenic mice, HIV43, 51 and 73, showed no proteinuria and normal renal histology. Transgenic offspring obtained by mating HIV43 or HIV73 with FVB/N or C57BL/6 mice showed normal renal histology without proteinuria. No offspring was obtained from HIV51.

Expression of the transgene

We analyzed transgene expression by RT-PCR using primers, nef3 and nef4, or nef6 and nef8, on polyA RNA extracted from the kidney. In transgenic mice of lines 13 and 34, and the HIV51 and HIV52 founder mice, the transgene mRNA was readily detected. However, in transgenic mice of lines 43 and 73, transgene expression was only marginally detectable by RT-PCR (Fig. 1B) (Table 2). As expected from the podocyte-specific activity of the nephrin promoter, the transgene mRNA was not detected in other organs, including the liver, spleen, intestine, colon, heart, and lung (data not shown).

Northern blot analysis confirmed that HIV-1 RNA was expressed in the kidneys of transgenic mice of lines 13 and 34, and the HIV51 and HIV52 founder mice, but not in wild-type mice or transgenic mice of lines 43 and 73 (Fig. 1C). The size of the main transcript was about 3 kb. HIV52, which expressed the highest level of HIV-1 RNA, showed an additional larger transcript.

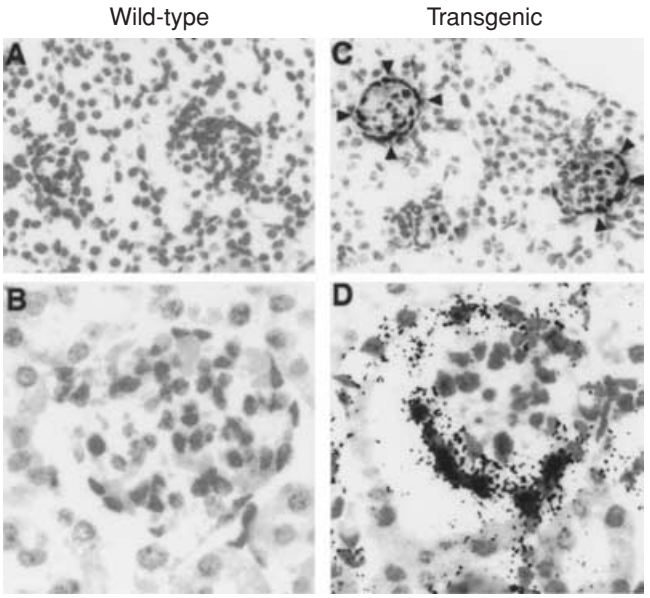

Fig. 2. In situ hybridization for HIV-1 mRNA in HIV13 mice. HIV-1 mRNA was localized to the periphery of the glomeruli [i.e., on podocytes in transgenic mice (*C*, arrowheads, and *D*)], whereas it was not detectable in wild-type mice (*A* and *B*). Sense probe showed no significant signals (not shown) [(A and C) low magnification (×200); (B and D) high magnification (×400)].

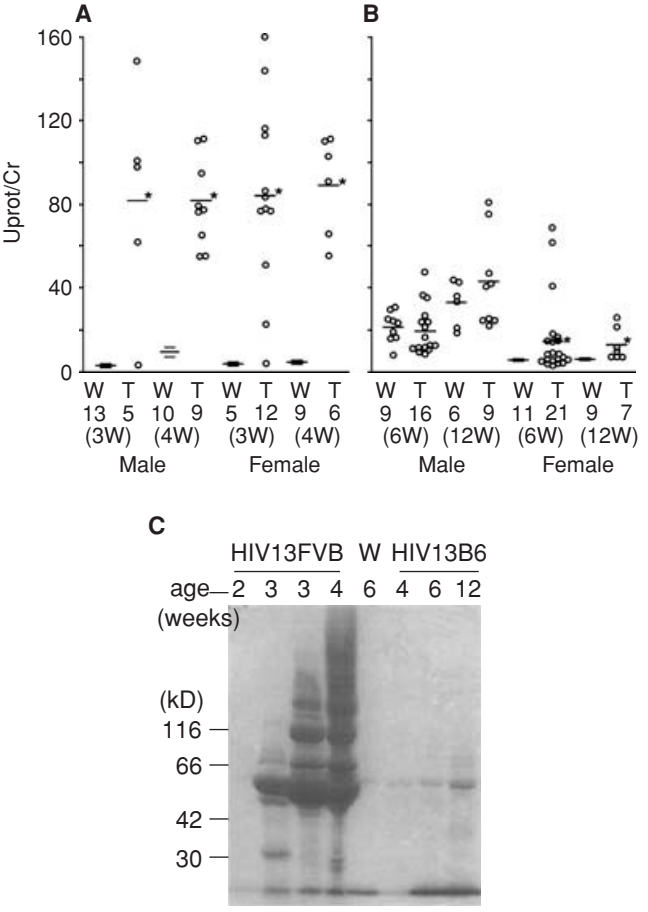

Fig. 3. Proteinuria in HIV13 mice. (*A* and *B*) The ratio of total urinary protein (mg/mL) to urinary creatinine (mg/mL) (Uprot/Cr) was determined with 24-hour urine samples from (A) HIV13FVB and (B) HIV13B6 mice. T, transgenic mice; W, wild-type mice. $^*P < 0.05$ vs. wild-type. Mean values (long bars) ± SE (short bars) are shown for male wild-type mice at 3 and 4 weeks of age and female wild-type mice at all ages. For transgenic mice and older wild-type males, individual measurements (○) and mean values (–) are shown. Numbers above the age represent the number of mice examined. (*C*) Sodium dodecyl sulfate-polyacrylamide gel electrophoresis (SDS-PAGE) analysis of urinary protein. Urine samples (2 μL) from HIV13FVB, HIV13B6 and wild-type (W) mice were analyzed at the ages indicated.

We further analyzed RNA of transgenic offspring of the founder mice HIV13 by RT-PCR using various primers listed in Table 1. As shown in Figure 1A, mRNAs for *vif*, *vpr*, *tat*, *rev*, and *nef,* but not *vpu,* were detected. mRNAs of *tat* and *rev* were spliced at nt 6044 and nt 8369, and unspliced forms were not detected.

The level of viral protein expression was below that detectable by immunostaining using antibodies against NEF, TAT, VPR, REV, or VIF. In situ hybridization performed on the kidneys of line HIV13 transgenic mice revealed that HIV-1 RNA expression was confined within the glomerulus. It was localized to the periphery of the glomerular capillary tuft corresponding to podocytes, but not along Bowman's capsule (Fig. 2). No specific signal was detected with the sense probe.

Nephrotic syndrome and survival in HIV13FBV vs. wild-type mice

Most HIV13FVB mice developed proteinuria around 3 weeks of age (Fig. 3A). SDS-PAGE analysis of the urine showed that proteinuria was non-selective (Fig. 3C). We longitudinally followed 14 HIV13FBV mice and 14 wild-type littermates. After 3 weeks of age, HIV13FVB mice showed growth retardation. The mean body weight of HIV13FVB was less than 80% of that of wild-type littermates at 4 weeks of age. They began to die after 4 weeks of age and exhibited 71% mortality within 18 weeks (Fig. 4). Two of the 4 HIV13FVB mice that survived for 18 weeks also showed proteinuria and nephropathy on histologic analysis. The penetrance rate of the nephropathy in this study was 86%. No wild-type littermates showed abnormality. Some HIV13FVB mice showed a small amount of ascites before the death. At 3 weeks of age, blood urea nitrogen (BUN) was elevated to 154.0 ± 50.9 mg/dL in HIV13FVB mice ($N = 6$) vs. 18.6 ± 1.7 mg/dL in wild-type littermates ($N = 6$) ($P < 0.05$).

Genetic predisposition to nephropathy

In contrast to HIV13FVB mice, most HIV13B6 mice showed no or only mild and slowly progressive nephropathy. Since mature wild-type male mice excrete a relatively high amount of protein in urine, the incidence of proteinuria was assessed in female mice. Only three of the

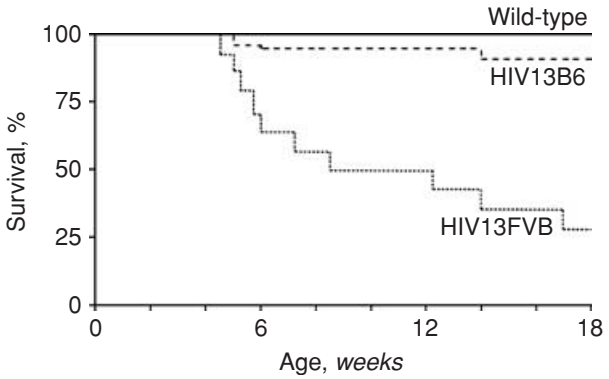

Fig. 4. Survival rates for HIV13FVB and HIV13B6 mice. HIV13FVB mice ($N = 14$), their wild-type littermates ($N = 14$), HIV13B6 mice ($N = 55$), and their wild-type littermates ($N = 50$) were longitudinally followed up to 18 weeks of age. No mice died in either wild-type group, over the time span. Ten HIV13FVB mice died by 18 weeks of age, and they all showed severe glomerulosclerosis. Of the four HIV13FVB mice that survived for 18 weeks, two showed moderate focal segmental glomerulosclerosis (FSGS), and the other two showed normal renal histology.

Table 3. Glomerular maturity indices in HIV13FVB and wild-type littermates at 2 weeks of age

Genotype	Transgenic (HIV13FVB) ($N = 4$)	Wild-type ($N = 5$)	P value
Total cortex	1.42 ± 0.02	1.54 ± 0.07	<0.05
Outer cortex	1.28 ± 0.04	1.40 ± 0.10	<0.05
Inner cortex	1.56 ± 0.03	1.66 ± 0.05	<0.05

21 (14%) HIV13B6 female mice showed overt nonselective proteinuria, and five HIV13B6 mice showed mild albuminuria by 6 weeks of age (Fig. 3B and C). Of the 55 HIVB6 mice followed longitudinally for 18 weeks, only four mice died between 4 and 13 weeks of age (Fig. 4).

When HIV13B6 mice were backcrossed with C57BL/6 mice three more times, none of the transgenic offspring ($N = 12$) developed nephropathy by 10 months of age. When the backcrossed mice were mated again with FVB/N mice, 10 out of 12 transgenic offspring developed severe nephropathy by 6 weeks of age.

Renal lesions in HIV13FVB mice

Before the appearance of proteinuria, no glomerular damage was observed in HIV13FVB mice by light microscopy. In wild-type mice, glomerular maturation was completed after 3 weeks of age. However, in HIV13FVB mice around the onset of proteinuria, glomeruli were often found to have reduced branching of capillaries. We semiquantified the glomerular maturation in 2 weeks old HIV13FVB mice (0 to 3+ score) (Table 3). In both the inner and outer cortices, the glomerular maturity score in HIV13FVB mice was significantly lower than that in wild-type littermates.

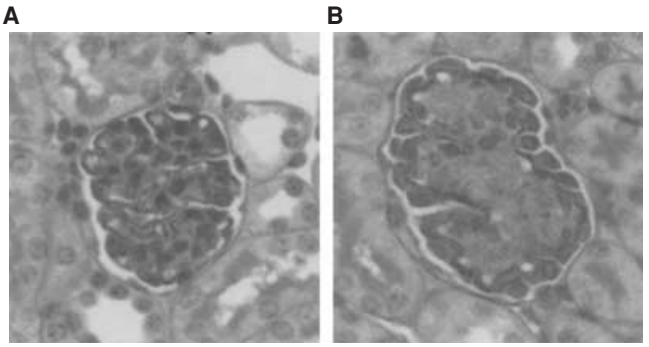

Fig. 5. Glomerular morphology around the onset of proteinuria. Wild-type (*A*) and HIV13FVB (*B*) at 3 weeks of age. Glomeruli in HIV13FVB mice often showed decreased branching of capillaries, and cuboidal-shaped podocytes [synaptopodin and periodic acid-Schiff (PAS) staining ×400].

In addition to the immaturity of the glomerular structure, podocytes also showed immature morphology in HIV13FVB mice. In mature glomeruli of wild-type mice, podocyte cell bodies were mature with extended cytoplasm along the basement membrane. In contrast, more than 50% of glomeruli of HIV13FVB mice showed cuboidal podocytes with plump undifferentiated cell bodies as opposed to flat cell bodies of differentiated podocytes. Cuboidal podocytes were observed until shortly after the onset of proteinuria (Fig. 5) before podocytes were damaged.

Electron microscopy at 3 weeks of age in HIV13FVB mice showed podocyte degeneration with vacuoles and blunted or completely effaced foot processes. The lamina rara externa, but not interna, of the glomerular basement membrane (GBM) exhibited an abnormal scalloped appearance. In some severely damaged glomeruli, there were subendothelial electron-dense deposits. Endothelial cells were abnormally swollen. Mesangial cells were increased in number, and early mesangiolysis was occasionally observed. Parietal epithelial cells and proximal tubular cells lining Bowman's capsule were injured with vacuolar changes and occasional necrosis (Fig. 6A).

To analyze the morphology of podocytes further in detail, we observed kidney tissues with scanning electron microscopy at 3 weeks of age (Fig. 6B and C). In wild-type glomeruli, podocytes had fully developed primary processes, with full development of secondary processes, and the GBM was covered by mature foot processes. In glomeruli of HIV13FVB mice, most surface areas of the GBM were covered by cuboidal podocyte cell bodies and the area covered by foot processes was markedly reduced. Moreover, numerous microvilli were observed on the surface of podocytes.

In contrast, HIV13B6 mice showed no immaturity of glomerular architecture or podocyte morphology.

After the onset of proteinuria, most remarkable changes were vacuolar degeneration of podocytes and

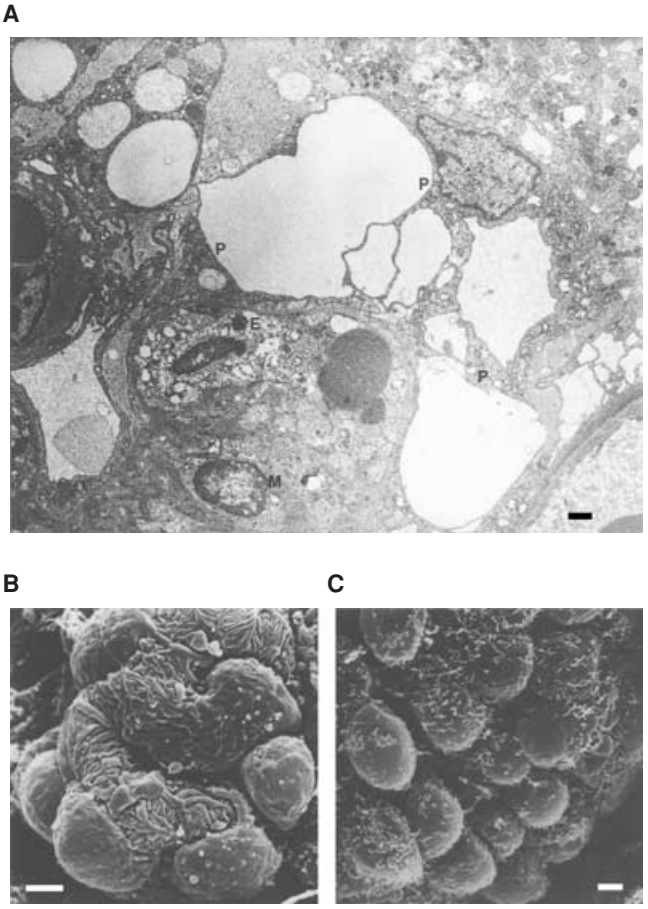

Fig. 6. Glomerular structure at 3 weeks of age. (*A*) Transmission electron microscopy of the kidneys of HIV13FVB mice. Podocytes (P) showed degeneration with huge vacuoles, with complete effacement of foot processes. The glomerular basememnt membrane was irregularly scalloped. Endothelial cells (E) were swollen. M is mesangial cell. Bars represent 1 μm. (*B* and *C*) Scanning electron microscopy of the glomeruli from wild-type (B) and HIV13FVB (C) mice. In wild-type mice, primary processes and foot processes of podocytes were well developed, whereas in HIV13FVB mice, only podocyte cell bodies, with microvillous transformation, were observed. Bars represent 1 μm.

parietal epithelial cells (Figs. 7D and 8F). Both flat and proximal tubular cell-type parietal epithelial cells were affected. Podocytes and parietal epithelial cells often contained protein reabsorption droplets, adhered to each other and were intermingled. Immunostaining revealed that synaptopodin and WT-1, markers for podocytes, were markedly reduced in damaged glomeruli (Fig. 8H and I). Some podocytes stained positive for desmin, a marker of damaged podocytes (Fig. 8J and K).

Glomerular epithelial cells proliferated and filled Bowman's space. In some glomeruli, they formed fibrocellular crescents. Most of these cells in Bowman's space, except for those directly attached to the GBM, stained positive for cytokeratin, a marker of parietal epithelial cells, but not for synaptopodin, a marker of podocytes (Fig. 8G and H). Some cytokeratin-positive and desmin-negative cells were located on the outer surface of the GBM (Fig. 8K and L). Cytokeratin and desmin staining did not overlap each other (i.e., no glomerular cells was doubly positive). Ki-67 positivity, a proliferation marker cell, was mainly present in parietal epithelial cells (Fig. 9B). Although rare, cytokeratin-negative and synaptopodin-positive podocytes piled up forming two layers in some glomeruli of young HIV13FVB mice, while parietal epithelial cells appeared quite quiescent (Fig. 9C and D). However, Ki-67 was not detected in these cells, indicating that they were not in proliferating phase at the time of sacrifice.

Soon after the onset of proteinuria, expansion of mesangial matrix, with an increase in collagen (data not shown), was observed and intensified with time. In some mice, mesangial hyperplasia was observed. After 4 weeks of age, HIV13FVB mice developed glomerulosclerosis (Figs. 7D and 10B) with focal segmental collapse. In the later phase of disease progression, mesangial matrix contained intensely periodic acid-Schiff (PAS)–positive materials, which often stained positive for IgG, IgM, and fibrinogen (data not shown).

In parallel with proteinuria, proteinaceous casts accumulated in tubular lumens. After 6 weeks of age, HIV13FVB mice showed interstitial fibrosis and diffuse tubular dilatation with focal microcystic lesions (Fig. 7C). Tubular and interstitial cells in HIV13FVB mice showed more intensive proliferation than glomerular cells, indicated by Ki-67 staining (Fig. 9B), and apoptosis, as depicted by terminal deoxynucleotidyl transferase (TdT)-mediated deoxyuridine triphosphate (dUTP) nick end labeling (TUNEL) staining (data not shown).

Renal lesions in HIV13B6 mice

Most HIV13B6 mice survived more than 6 months after birth. Of the 12 HIV13B6 mice histologically analyzed after 6 months of age, four (33%) were completely normal. Two showed advanced FSGS and tubular dilatation and interstitial fibrosis. The other six mice (50%) showed focal intratubular casts and mild mesangial expansion and, occasionally, glomerular sclerosis (Fig. 7E and F). No HIV13B6 mice showed collapsing FSGS lesions or vacuolar degeneration of podocytes.

DISCUSSION

In the present study, we generated transgenic mice that express nonstructural HIV-1 genes selectively in podocytes. The transgenic mice showed injury not only in podocytes but also in other renal cells, developed collapsing FSGS and microcystic tubular dilatation and died from renal failure.

Four of the seven transgenic mice subjected to analysis developed collapsing FSGS in the founders or their

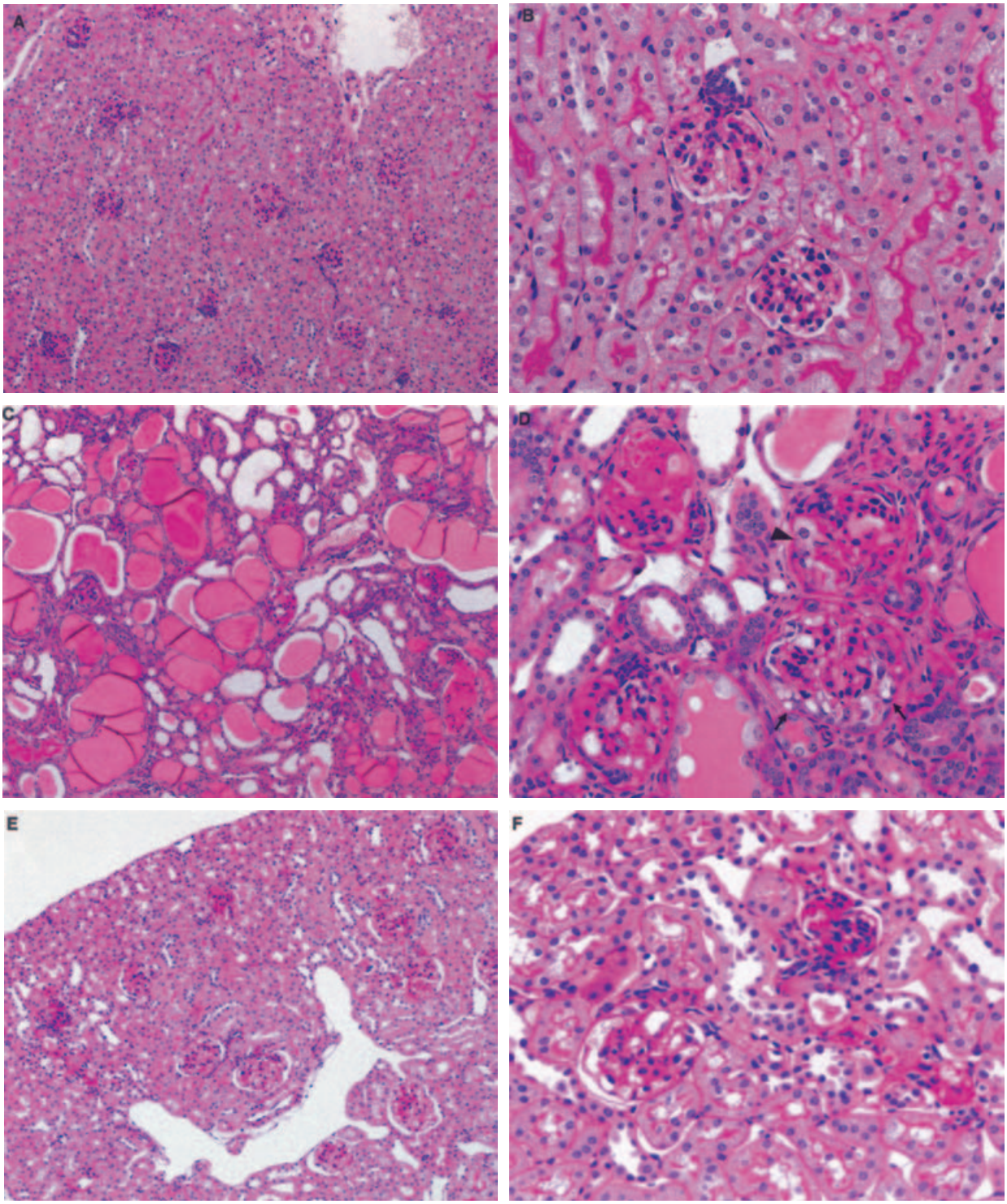

Fig. 7. Renal lesions of HIV13 transgenic mice. (*A* and *B*) Wild-type littermates of HIV13FVB mice at 6 weeks of age showed normal histology. (*C* and *D*) HIV13FVB mice at 6 weeks of age showed microcystic dilatation of tubules (C) and global or segmental glomerulosclerosis, collapsing glomerulosclerosis (D, arrow), and vacuolar degeneration of glomerular epithelial cells (D, arrowheads). (*E* and *F*) HIV13B6 mice at 6 months of age showed focal segmental glomerulosclerosis (FSGS) and mesangial expansion [periodic acid-Schiff (PAS) staining ×100 (A, C, and E) and ×200 (B, D, and F)].

offspring. Two factors should be considered regarding the incomplete penetrance of nephropathy. First, the penetrance rate of transgene expression by the nephrin promoter is not always 100%. Thus far, we have generated several other transgenic mice and observed that the rate of renal expression of the transgene ranged from about 20% to 80% [47] (unpublished observations). A second key factor is genetic background. The development

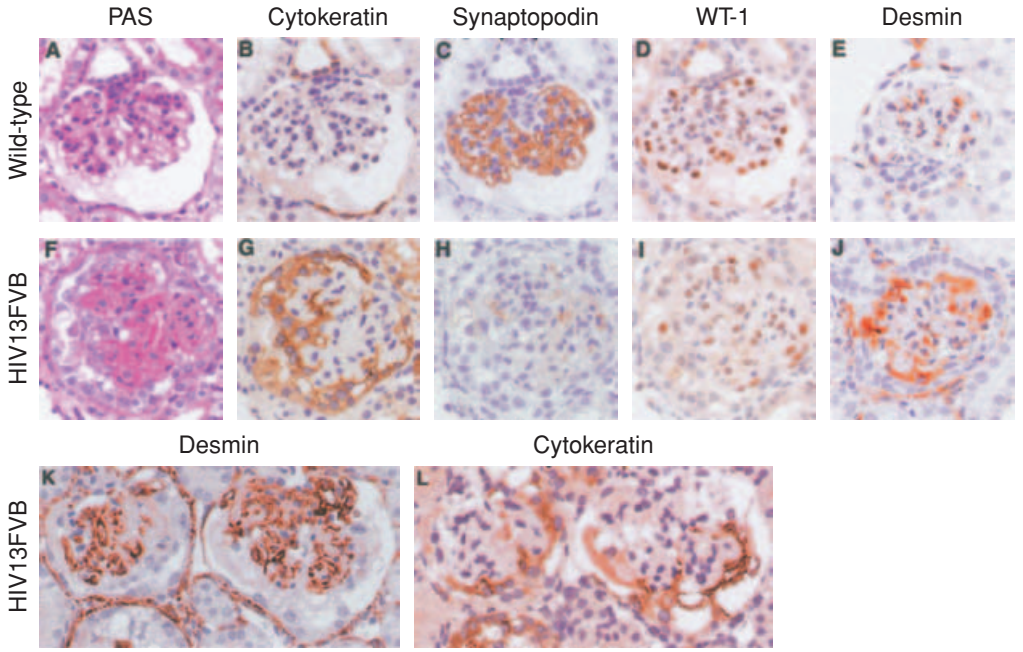

Fig. 8. Damage of glomerular epithelial cells in HIV13FVB mice. Wild-type (*A* to *E*) and HIV13FVB (*F* to *L*) mice at 4 weeks of age. Note the prominent proliferation and degeneration of epithelial cells with cytokeratin immunoactivity, a marker for parietal epithelial cells, with markedly reduced synaptopodin and WT-1, podocyte markers (F to I vs. A to D). In wild-type mice, desmin was faintly detectable only in mesangial cells (E), whereas in HIV13FVB mice, desmin was expressed in podocytes (J). Staining for desmin (K) and cytokeratin (L) in adjacent sections revealed that some visceral epithelial cells were negative for desmin and positive for cytokeratin. No cells were doubly positive for desmin and cytokeratin [periodic acid-Schiff (PAS) staining (A and F) and immunostaining for cytokeratin (B, G, and L), synaptopodin (C and H), WT-1 (D and I) or desmin (E, J, and K) (A to E, E to F, K and L, respectively, are adjacent sections (×400)].

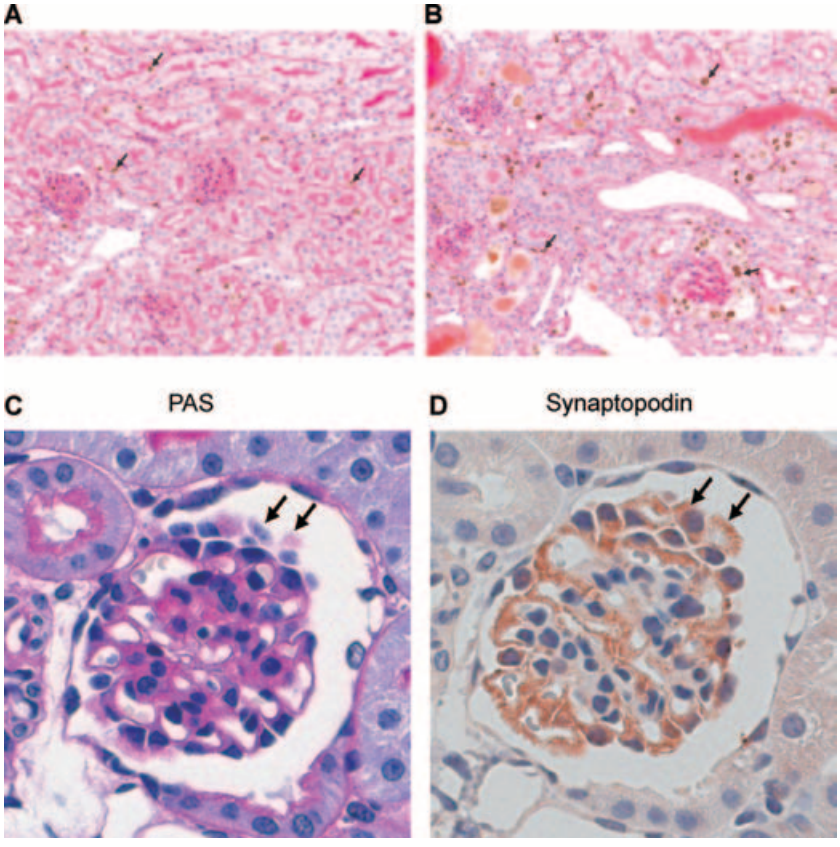

Fig. 9. Cell proliferation in wild-type and HIV13FVB mice. (*A* and *B*) In wild-type mice (A), a rare Ki-67 staining is indicated with arrows. Ki-67 in tubular and glomerular parietal epithelial cells was increased in HIV13FVB mice (B). Immunostaining for Ki-67 with counterstaining by periodic acid-Schiff (PAS) in wild-type (A) and HIV13FVB mice (B) (×200). (*C* and *D*) Apparent proliferation of podocytes in HIV13FVB mice. In some glomeruli of HIV13FVB mice, podocytes piled up, forming two layers. PAS (C) and synaptopodin (D) staining in the adjacent section (×400).

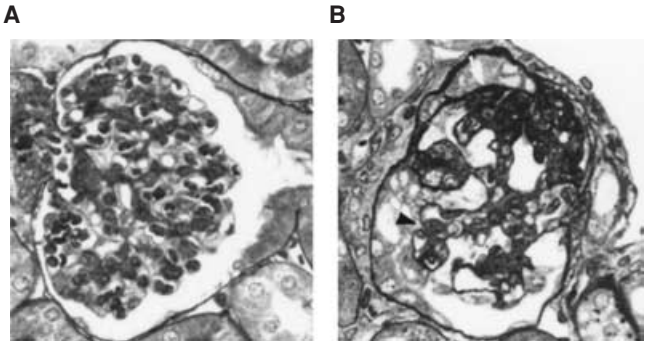

Fig. 10. Glomerulosclerosis in wild-type and HIV13FVB mice. Wild-type (*A*) and HIV13FVB (*B*) mice at 4 weeks of age. In HIV13FVB mice (B), glomeruli show noncollapsing segmental sclerosis (arrow) and collapsing sclerosis (arrowhead) [silver staining (×400)].

of nephropathy in the Tg26 line highly depends on the FVB genetic background [48]. The founder transgenic mice of the present study had a mixed genetic background of C57BL/6 and DBA/2, both of which are resistant to Tg26-induced nephropathy. Of the three transgenic mice that did not show proteinuria, two mice did not express the transgene in the kidney. The other mouse expressed the transgene in the kidney, but was infertile, therefore, this line could not be analyzed on the FVB genetic background.

HIV-1 virus encodes nine genes. Among those genes, accumulating data indicate that *nef* and *vpr* are involved in the pathogenesis of HIVAN. HIV-1 transgenic animals lacking *pol* and gag develop renal lesions similar to HIVAN [23, 32, 34–37, 39, 41, 49]. Kajiyama et al [50] reported that a transgenic mouse line expressing HIV-1 genes lacking *gag*, *pol*, and *nef* under the control of its own promoter developed FSGS, and that genetic complementation with *nef* substantiated FSGS. Dickie et al [49] reported that transgenic mouse lines expressing *vpr* in the kidney, under the regulation of its own promoter or of the *c-fms* promoter, but not those lacking *vpr*, developed FSGS [49]. However, the CD4C/HIVtransgenic mice expressing *nef* with the CD4 regulatory elements also develop FSGS and interstitial nephritis [37, 45]. In addition, in vitro experiments showed that *nef* induces proliferation, anchorage-independent growth and dedifferentiation of podocytes [51, 52]. These results collectively indicate that *vpr* and *nef* can each induce FSGS. However, the pathogenicity of these two gene products may depend on the cell population in which they are expressed. Indeed, *vpr* could not induce nephropathy when expressed under the regulation of the CD4C promoter, while *nef* was very efficient at doing so [37]. Moreover, it appears that *nef* potentiates the development of glomerulosclerosis by *vpr* when expressed under the LTR promoter, possibly in podocytes. In the transgenic mice studied here, both *vpr* and *nef* were expressed in podocytes and may be collaborating to induce nephropathy, a notion consistent with the previous suggestions. Our transgenic mice do not carry *env*, *gag*, and *pol*, confirming that these viral gene products are not involved in the pathogenesis of HIVAN.

In our transgenic mice, we used a podocyte-specific nephrin promoter. Indeed, HIV-1 mRNA was detected in podocytes by in situ hybridization. As predicted, podocytes were severely injured in HIV13FVB mice. Podocyte injury was identified by light microscopy, transmission electron microscopy, scanning electron microscopy, and immunostaining. In addition, other glomerular cells, including mesangial cells, glomerular endothelial cells, and parietal epithelial cells, were also injured. Similar renal pathologies were observed in another podocyte-selective injury model (NEP25) that we recently developed [47]. NEP25 is a transgenic mouse line expressing human (h) CD25 selectively in podocytes. Injection of an immunotoxin specific to hCD25 allowed us to induce podocyte-specific injury. After the injection of the immunotoxin, NEP25 mice showed injuries not only in podocytes, but also in other glomerular cells, including endothelial cells, mesangial cells, and parietal epithelial cells, and developed glomerulosclerosis. In addition to glomerular damage, NEP25 mice developed tubulointerstitial injuries, including microcystic tubular dilatation. HIV13FVB mice and NEP25 mice share a number of similar pathologic features, namely vacuolization of podocytes and parietal epithelial cells, proliferation of parietal epithelial cells, expansion of mesangial matrix, mesangiolysis, swelling of glomerular endothelial cells, hyalinosis, glomerular sclerosis, deposition of immunoglobulins in a later phase, and tubulointerstitial injuries. These phenotypes, therefore, appear to be the common outcomes triggered by podocyte injury. On the other hand, collapse of glomerular capillaries, immature morphology of the glomerulus and podocytes and rare proliferation of podocytes were unique to HIV13 transgenic mice.

Similar to Tg26 mice, HIV13FBV mice showed avid cell proliferation within Bowman's space. These extracapillary proliferating cells and parietal epithelial cells lining Bowman's capsule were often positive for Ki-67, whereas the cells adjacent to the GBM were rarely positive for Ki-67. Most cells proliferating distant from the GBM were positive for cytokeratin, a marker of parietal epithelial cells. Synaptopodin, when it was not completely down-regulated, was detected only in cells adjacent to the GBM. We found no cells doubly positive for synaptopodin and Ki-67. These findings indicate that most cells proliferating in Bowman's space were derived from parietal epithelial cells, as suggested in some studies on human nephropathy [53, 54]. The possibility, however, cannot be ruled out that podocytes changed phenotype and also acquired proliferative capability. In fact, although

very rare, we identified occasional podocytes by synaptopodin staining that had piled up and formed two layers, suggesting podocyte proliferation. Some desmin-negative and cytokeratin-positive cells were located on the outer surface of the GBM. Despite extensive search, we found no cells doubly positive for desmin and cytokeratin. These indicate that parietal epithelial cells may migrate and locate at the visceral site, rather than that podocytes undergo phenotypic transition.

The reason why podocyte proliferation was rare in HIV13FVB mice remains unclear. The possibility exists that the expression of HIV-1 transgene, driven by the nephrin promoter, may be quickly down-regulated when podocytes change their phenotype. In fact, HIV-1 mRNA was not detected by RT-PCR in kidneys with severe lesions (data not shown). Likewise, studies in Tg26 mice showed that HIV-1 transgene expression, driven by the authentic HIV-1 promoter, LTR, was down-regulated in the end stage of the disease [32]. The timing and extent of down-regulation of the promoter may cause different phenotypes regarding podocyte hyperplasia.

Around the onset of proteinuria, podocytes of HIV13FVB mice showed a pattern of morphologic immaturity along with scalloped GBM. Although not a typical finding in HIVAN, scalloped GBM has been observed in some pediatric kidneys transplanted into adults [55]. Changes in hemodynamics or growth, that occurred when the small immature kidney is transplanted into the adult, may cause these unusual lesions. The immature podocytes were devoid of extension of primary processes and foot processes. This observation, together with the fact that HIV-1 proteins, including Nef and Vpr, can associate with cytoskeleton and alter cell shape, lead us to the following speculation on the development of renal lesions in HIV13FVB mice. HIV-1 gene products may affect the cytoskeleton or other cellular components and inhibit the projection of processes. This abnormality of podocytes may in turn cause decreased branching of glomerular capillaries, a lesion often observed in HIV13FVB mice. These abnormal podocytes also cannot function as an effective filtration barrier, resulting in massive proteinuria. Proteinuria, or other abnormalities that occur after the onset of proteinuria, may cause secondary damage to podocytes and other renal cells as seen in NEP25 mice, ultimately leading to glomerulosclerosis.

In addition to glomerular damage, HIV13FVB mice also developed tubulointerstitial injuries, similar to NEP25 mice [47]. In a later phase, tubular microcystic lesions developed. In human kidneys with HIVAN or those of Tg26 mice, but not in CD4C/HIV transgenic mice, HIV-1 DNA and RNA were detected in tubular cells [25–27, 38, 42]. Bruggeman et al [34] reported that up-regulation of the transgene by ultraviolet light irradiation-induced apoptosis of tubular cells in cultured renal tissues of Tg26 mice, indicating that HIV-1 gene products have direct toxic effects on renal tubular cells. In this regard, our present observations with podocyte-restricted expression of HIV-1 genes suggest that the tubular and interstitial alterations in HIV13FVB mice, quite like those in NEP25 mice, are secondary to glomerular deterioration triggered by podocyte injury, and further verify the capacity of podocyte injury to bring about the progression of HIVAN.

Development of HIVAN in HIV-1 infected patients shows a strong racial predilection for black and Hispanic patients. Similarly, the development of nephropathy in Tg26 line is highly dependent on FVB/N genetic background, although the transgene expression level is not enhanced by FVB/N genetic background. The locus for the susceptibility to nephropathy in mice has been mapped to chromosome 3A1-3 [48]. Development of nephropathy in the HIV13 line also showed a strong genetic predilection for FVB/N genetic background. Thus, the founder HIV13 had, on average, 75% of C57BL/6 and 25% of DBA/2 genetic background, and showed very mild renal lesions without overt proteinuria. Most HIV13FVB mice showed severe nephropathy after 3 weeks of age, while most HIV13B6 mice showed either no or very mild renal lesions. When HIV13B6 mice were further backcrossed with C57BL/6 mice four times, none of the transgenic offspring showed abnormality in the kidney. These findings indicate that irrespective of the promoter driving HIV-1 genes, FVB/N genetic background enhances the progression of the renal disease caused by HIV-1 gene products.

Some HIV13B6 mice showed mild and less progressive renal lesions. These lesions mainly consisted of mesangial changes, and no vacuolar degeneration of podocytes was observed. We also observed a similar phenomenon in NEP25 mice injected with a small dose of immunotoxin [47]. In these NEP25 mice, the main lesion was mesangial expansion, and vacuolization of podocytes was less remarkable. Interestingly, mesangial change is frequently observed in HIVAN, especially in children, and HIV-1–infected patients with mesangial lesions show a slower rate of the progression of the renal disease than those with FSGS [30]. It is conceivable that HIV-1-induced podocyte dysregulation is the central mechanism of the full spectrum of HIVAN, whereas the above atypical renal complications develop under the influence of genetic factors.

CONCLUSION

We demonstrate that the expression of HIV-1 genes selectively in podocytes alone is sufficient for the development of the full spectrum of typical and atypical HIVAN.

ACKNOWLEDGMENTS

We thank Ms. Niwa, Ms. Sato, Ms. Sakurai, Ms. Sasaoka, Ms. Donnert, Mr. Akatsuka, and Mr. Tokunaga for technical assistance, Mr. Homma and Ms. Inoue for editorial assistance, Dr. Hataba for kind

instruction for SEM and Dr. Niimura and Dr. Kurihara for valuable discussions. This study was supported by NIH grants DK37868, DK44757, USA, the Research for the Future Program and Grant-in Aid for Scientific Research of Japan Society for the Promotion of Science, and MEXT. HAITEKU (2002–2006) . A part of this study was presented in abstract form at the annual meeting of the American Society of Nephrology in 2003.

Reprint requests to Taiji Matsusaka, Departments of Pediatrics, Vanderbilt University Medical Center, MCN C4204, Nashville, TN37232-3584.
E-mail: matsusaka_taiji@yahoo.com

REFERENCES

1. Kestila M, Lenkkeri U, Mannikko M, *et al*: Positionally cloned gene for a novel glomerular protein—nephrin—is mutated in congenital nephrotic syndrome. *Mol Cell* 1:575–582, 1998
2. Kim YH, Goyal M, Kurnit D, *et al*: Podocyte depletion and glomerulosclerosis have a direct relationship in the PAN-treated rat. *Kidney Int* 60:957–968, 2001
3. Kriz W, Gretz N, Lemley KV: Progression of glomerular diseases: Is the podocyte the culprit? *Kidney Int* 54:687–697, 1998
4. Rennke HG: How does glomerular epithelial cell injury contribute to progressive glomerular damage? *Kidney Int* (Suppl 45):S58–S63, 1994
5. Ross MJ, Klotman PE: Recent progress in HIV-associated nephropathy. *J Am Soc Nephrol* 13:2997–3004, 2002
6. Boute N, Gribouval O, Roselli S, *et al*: NPHS2, encoding the glomerular protein podocin, is mutated in autosomal recessive steroid-resistant nephrotic syndrome. *Nat Genet* 24:349–354, 2000
7. Kaplan JM, Kim SH, North KN, *et al*: Mutations in ACTN4, encoding alpha-actinin-4, cause familial focal segmental glomerulosclerosis. *Nat Genet* 24:251–256, 2000
8. Kim JM, Wu H, Green G, *et al*: CD2-associated protein haploinsufficiency is linked to glomerular disease susceptibility. *Science* 300:1298–1300, 2003
9. Kos CH, Le TC, Sinha S, *et al*: Mice deficient in alpha-actinin-4 have severe glomerular disease. *J Clin Invest* 111:1683–1690, 2003
10. Pollak MR: Inherited podocytopathies: FSGS and nephrotic syndrome from a genetic viewpoint. *J Am Soc Nephrol* 13:3016–3023, 2002
11. Shih NY, Li J, Karpitskii V, *et al*: Congenital nephrotic syndrome in mice lacking CD2-associated protein. *Science* 286:312–315, 1999
12. Roselli S, Heidet L, Sich M, *et al*: Early glomerular filtration defect and severe renal disease in podocin-deficient mice. *Mol Cell Biol* 24:550–560, 2004
13. Kerjaschki D: Caught flat-footed: Podocyte damage and the molecular bases of focal glomerulosclerosis. *J Clin Invest* 108:1583–1587, 2001
14. Mundel P, Shankland SJ: Podocyte biology and response to injury. *J Am Soc Nephrol* 13:3005–3015, 2002
15. Pavenstadt H, Kriz W, Kretzler M: Cell biology of the glomerular podocyte. *Physiol Rev* 83:253–307, 2003
16. Bourgoignie JJ: Renal complications of human immunodeficiency virus type 1. *Kidney Int* 37:1571–1584, 1990
17. Humphreys MH: Human immunodeficiency virus-associated glomerulosclerosis. *Kidney Int* 48:311–320, 1995
18. Kimmel PL, Barisoni L, Kopp JB: Pathogenesis and treatment of HIV-associated renal diseases: Lessons from clinical and animal studies, molecular pathologic correlations, and genetic investigations. *Ann Intern Med* 139:214–226, 2003
19. Klotman PE: HIV-associated nephropathy. *Kidney Int* 56:1161–1176, 1999
20. Ross MJ, Klotman PE: HIV-associated nephropathy. *Aids* 18:1089–1099, 2004
21. Weiner NJ, Goodman JW, Kimmel PL: The HIV-associated renal diseases: Current insight into pathogenesis and treatment. *Kidney Int* 63:1618–1631, 2003
22. Barisoni L, Kriz W, Mundel P, *et al*: The dysregulated podocyte phenotype: A novel concept in the pathogenesis of collapsing idiopathic focal segmental glomerulosclerosis and HIV-associated nephropathy. *J Am Soc Nephrol* 10:51–61, 1999
23. Barisoni L, Mokrzycki M, Sablay L, *et al*: Podocyte cell cycle regulation and proliferation in collapsing glomerulopathies. *Kidney Int* 58:137–143, 2000
24. Shankland SJ, Eitner F, Hudkins KL, *et al*: Differential expression of cyclin-dependent kinase inhibitors in human glomerular disease: Role in podocyte proliferation and maturation. *Kidney Int* 58:674–683, 2000
25. Bruggeman LA, Ross MD, Tanji N, *et al*: Renal epithelium is a previously unrecognized site of HIV-1 infection. *J Am Soc Nephrol* 11:2079–2087, 2000
26. Ross MJ, Bruggeman LA, Wilson PD, *et al*: Microcyst formation and HIV-1 gene expression occur in multiple nephron segments in HIV-associated nephropathy. *J Am Soc Nephrol* 12:2645–2651, 2001
27. Winston JA, Bruggeman LA, Ross MD, *et al*: Nephropathy and establishment of a renal reservoir of HIV type 1 during primary infection. *N Engl J Med* 344:1979–1984, 2001
28. Marras D, Bruggeman LA, Gao F, *et al*: Replication and compartmentalization of HIV-1 in kidney epithelium of patients with HIV-associated nephropathy. *Nat Med* 8:522–526, 2002
29. Nochy D, Glotz D, Dosquet P, *et al*: Renal disease associated with HIV infection: A multicentric study of 60 patients from Paris hospitals. *Nephrol Dial Transplant* 8:11–19, 1993
30. Ray PE, Xu L, Rakusan T, *et al*: A 20-year history of childhood HIV-associated nephropathy. *Pediatr Nephrol* 19:1075–1092, 2004
31. Dickie P, Felser J, Eckhaus M, *et al*: HIV-associated nephropathy in transgenic mice expressing HIV-1 genes. *Virology* 185:109–119, 1991
32. Kopp JB, Klotman ME, Adler SH, *et al*: Progressive glomerulosclerosis and enhanced renal accumulation of basement membrane components in mice transgenic for human immunodeficiency virus type 1 genes. *Proc Natl Acad Sci USA* 89:1577–1581, 1992
33. Barisoni L, Bruggeman LA, Mundel P, *et al*: HIV-1 induces renal epithelial dedifferentiation in a transgenic model of HIV-associated nephropathy. *Kidney Int* 58:173–181, 2000
34. Bruggeman LA, Dikman S, Meng C, *et al*: Nephropathy in human immunodeficiency virus-1 transgenic mice is due to renal transgene expression. *J Clin Invest* 100:84–92, 1997
35. Ray PE, Liu XH, Robinson LR, *et al*: A novel HIV-1 transgenic rat model of childhood HIV-1-associated nephropathy. *Kidney Int* 63:2242–2253, 2003
36. Reid W, Sadowska M, Denaro F, *et al*: An HIV-1 transgenic rat that develops HIV-related pathology and immunologic dysfunction. *Proc Natl Acad Sci USA* 98:9271–9276, 2001
37. Hanna Z, Kay DG, Rebai N, *et al*: Nef harbors a major determinant of pathogenicity for an AIDS-like disease induced by HIV-1 in transgenic mice. *Cell* 95:163–175, 1998
38. Simard MC, Chrobak P, Kay DG, *et al*: Expression of simian immunodeficiency virus nef in immune cells of transgenic mice leads to a severe AIDS-like disease. *J Virol* 76:3981–3995, 2002
39. Hanna Z, Priceputu E, Kay DG, *et al*: In vivo mutational analysis of the N-terminal region of HIV-1 Nef reveals critical motifs for the development of an AIDS-like disease in CD4C/HIV transgenic mice. *Virology* 327:273–286, 2004
40. de Repentigny L, Lewandowski D, Jolicoeur P: Immunopathogenesis of oropharyngeal candidiasis in human immunodeficiency virus infection. *Clin Microbiol Rev* 17:729–759, 2004
41. Priceputu E, Rodrigue I, Chrobak P, *et al*: The Nef-mediated AIDS-like disease ofCD4C/HIV transgenic mice is associated with increased Fas/FasL expression on T cells and T cell death, but is not prevented in Fas, FasL, TNFR-1 and ICE deficient nor in Bcl2-expressing transgenic mice. *J Virol* 16:1–20, 2005
42. Hanna Z, Kay DG, Cool M, *et al*: Transgenic mice expressing human immunodeficiency virus type 1 in immune cells develop a severe AIDS-like disease. *J Virol* 72:121–132, 1998
43. Hanna Z, Rebai N, Poudrier J, *et al*: Distinct regulatory elements are required for faithful expression of human CD4 in T cells, macrophages, and dendritic cells of transgenic mice. *Blood* 98:2275–2278, 2001
44. Hanna Z, Simard C, Laperriere A, *et al*: Specific expression of

the human CD4 gene in mature CD4+ CD8- and immature CD4+ CD8+ T cells and in macrophages of transgenic mice. *Mol Cell Biol* 14:1084–1094, 1994
45. Heckmann A, Waltzinger C, Jolicoeur P, *et al*: IKK2 inhibitor alleviates kidney and wasting diseases in a murine model of human AIDS. *Am J Pathol* 164:1253–1262, 2004
46. Niimura F, Labosky PA, Kakuchi J, *et al*: Gene targeting in mice reveals a requirement for angiotensin in the development and maintenance of kidney morphology and growth factor regulation. *J Clin Invest* 96:2947–2954, 1995
47. Matsusaka T, Xin J, Niwa S, *et al*: Genetic engineering of glomerular sclerosis in the mouse via control of onset and of severity of podocyte-specific injury. *J Am Soc Nephrol* 16:1–20, 2005
48. Gharavi AG, Ahmad T, Wong RD, *et al*: Mapping a locus for susceptibility to HIV-1-associated nephropathy to mouse chromosome 3. *Proc Natl Acad Sci USA* 101:2488–2493, 2004
49. Dickie P, Roberts A, Uwiera R, *et al*: Focal glomerulosclerosis in proviral and c-fms transgenic mice links Vpr expression to HIV-associated nephropathy. *Virology* 322:69–81, 2004
50. Kajiyama W, Kopp JB, Marinos NJ, *et al*: Glomerulosclerosis and viral gene expression in HIV-transgenic mice: role of nef. *Kidney Int* 58:1148–1159, 2000
51. Husain M, Gusella GL, Klotman ME, *et al*: HIV-1 Nef induces proliferation and anchorage-independent growth in podocytes. *J Am Soc Nephrol* 13:1806–1815, 2002
52. Sunamoto M, Husain M, He JC, *et al*: Critical role for Nef in HIV-1-induced podocyte dedifferentiation. *Kidney Int* 64:1695–1701, 2003
53. Kihara I, Yaoita E, Kawasaki K, *et al*: Origin of hyperplastic epithelial cells in idiopathic collapsing glomerulopathy. *Histopathology* 34:537–547, 1999
54. Nagata M, Horita S, Shu Y, *et al*: Phenotypic characteristics and cyclin-dependent kinase inhibitors repression in hyperplastic epithelial pathology in idiopathic focal segmental glomerulosclerosis. *Lab Invest* 80:869–880, 2000
55. Nadasdy T, Abdi R, Pitha J, *et al*: Diffuse glomerular basement membrane lamellation in renal allografts from pediatric donors to adult recipients. *Am J Surg Pathol* 23:437–442, 1999